J|A|C|S COMMUNICATIONS

Published on Web 12/30/2008

Single-Molecule Observation of Photocatalytic Reaction in TiO_2 Nanotube: Importance of Molecular Transport through Porous Structures

Kazuya Naito, Takashi Tachikawa, Mamoru Fujitsuka, and Tetsuro Majima*

The Institute of Scientific and Industrial Research (SANKEN), Osaka University, Mihogaoka 8-1, Ibaraki, Osaka 567-0047, Japan

Received October 23, 2008; E-mail: majima@sanken.osaka-u.ac.jp

Nano- and mesoporous materials have attracted considerable attention because they can be used to produce adsorbents, delivery carriers, photonic devices, and (photo)catalysts.[1] Recently, mesoporous TiO_2 materials such as hollow spheres, opals, and nanotubes have been synthesized with the objective of designing an efficient photocatalyst having a high specific surface area and high molecular selectivity;[2] these materials can also find potential applications as the diffusion-controllable membranes[3a] and in dye-sensitized solar cells (DSSCs),[3bc] and water-splitting systems.[3d] In these applications, the performance of reagent molecules should be directly determined by their accessibility to the active sites for adsorption onto and reaction with the surfaces of materials. However, the structural disorders and agglomerates present in bulk samples often hinder efficient molecular transport.[2d−f] Furthermore, because conventional measurement methods cannot be used to observe and distinguish between (photo)catalytic reactions occurring on active sites distributed over the catalyst, the inherent properties can only be obtained as the ensemble mean of heterogeneities. Therefore, an improved technique for examining a single fragment of a porous material is strongly required.[4]

In this paper, we describe the single-molecule imaging of photocatalytic reactions in a porous TiO_2 nanotube using total internal reflection fluorescence microscopy (TIRFM). Our method is shown in Figure 1. A TiO_2 nanotube synthesized by the sol−gel template method has a porous structure containing a straight macropore (pore size: 100−150 nm) and mesopores between the anatase nanoparticles (pore size: 5−10 nm) (Figures S1 and S2, Supporting Information).[5] The photocatalytic activity of the porous structure is evaluated by the single-molecule counting of hydroxyl radicals (•OH) using a specific fluorescent probe, aminophenyl fluorescein (APF),[6a] because •OH is the principal reactive oxygen species (ROS) in photocatalytic oxidation owing to its high oxidation power.[6b] The •OH in the photocatalytic reaction can be generated by the reduction and/or photodecomposition of H_2O_2, which is formed via the reduction of O_2 by the conduction band and/or trapped electrons in TiO_2 (see Supporting Information for details, section 1). An experiment on a single TiO_2 nanotube is conducted by using a custom-made sample chamber; in this chamber, the same nanotube can be observed under different substrate solutions (Figure S3A, Supporting Information). Each TiO_2 nanotube placed in this chamber is completely irradiated with UV light (wavelength: 365 nm) and evanescent light produced by a CW Ar^+ laser (wavelength: 488 nm) to excite the nanotube and fluorescein, respectively (Figure S3B, Supporting Information). Thus, it is expected that the photocatalytic reaction will occur randomly on the entire nanotube.

Figure 2 shows the results of the single-molecule counting of •OH generated in a single TiO_2 nanotube under static conditions (i.e., without sample flow). The fluorescence intensity increased significantly immediately after UV irradiation (t > 60 s) with a 500 nM APF phosphate buffer solution (pH 7.4) used as the substrate (Figure 2A). In contrast, in the presence of DMSO as an •OH quencher, the increase in fluorescence was suppressed (Figure 2B). Additionally, the single-molecule fluorescence spectra of the fluorescence generated under UV irradiation are consistent with that of fluorescein in a bulk solution (Figure S4, Supporting Information). These results confirm that fluorescein was produced by •OH and not by the auto-oxidation of APF caused by the intense UV irradiation (Figure S6, Supporting Information). Interestingly, the fluorescence can be observed only within the time resolution (33 ms); this result suggests that the fluorescein generated in the pores rapidly diffused out of the nanotube to the bulk solution. Considering the fact that the fluorescence bursts occurred less frequently than the data acquisition rate, we can almost rule out the possibility that multiple fluorescein molecules were detected simultaneously. Figure 2C shows the histograms of the fluorescence

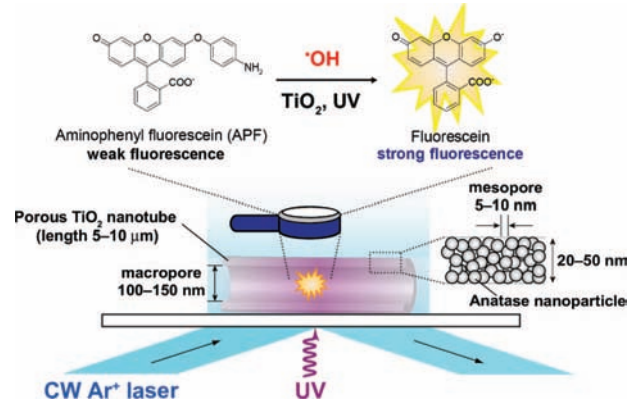

Figure 1. Schematic representation of photocatalytic reaction occurring on a single nanotube. (Top) Generation of emissive fluorescein induced by the photocatalytic reaction in the porous structure of the TiO_2 nanotube. (Bottom) The porous TiO_2 nanotube on the cover glass is simultaneously irradiated with UV light (wavelength: 365 nm) and evanescent light produced by a CW Ar^+ laser (wavelength: 488 nm) to excite the nanotube and fluorescein, respectively.

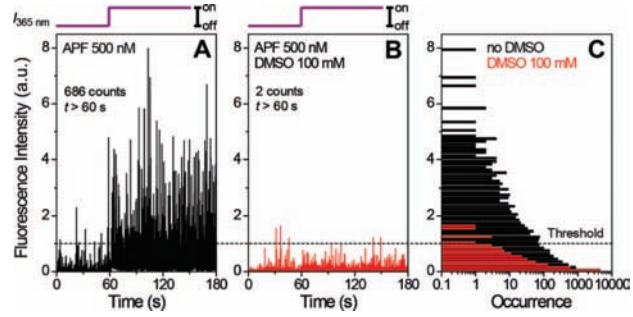

Figure 2. Time trajectories of the fluorescence intensity of the entire TiO_2 nanotube in the absence (A) and presence (B) of 100 mM DMSO as an •OH quencher. The histograms of the fluorescence intensity are also shown for comparison (C).

10.1021/ja808335b CCC: $40.75 © 2009 American Chemical Society

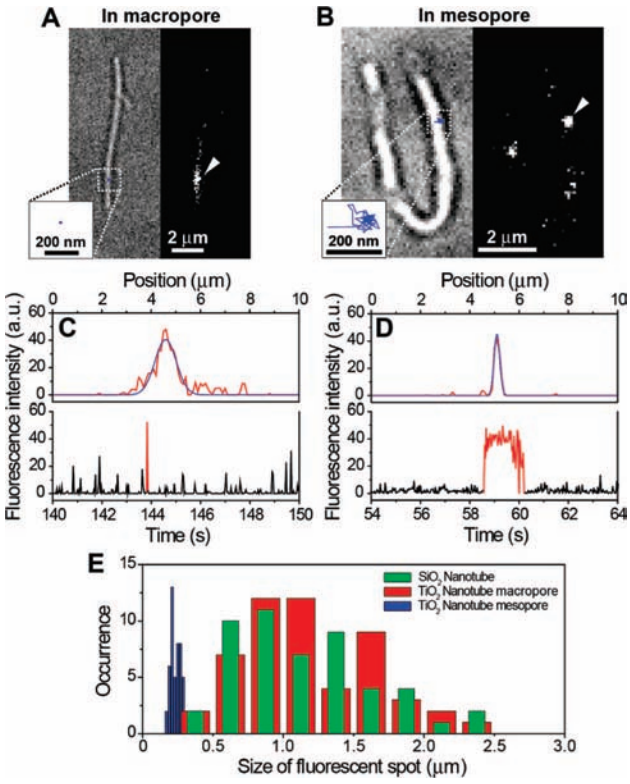

Figure 3. (A, B) Transmission image (left) and fluorescence image (right). Inset shows the peak trajectory of single-molecule fluorescence generated in the macropore (A) and mesopore (B) of the TiO_2 nanotube. (C, D) Line profile (upper panel) and time trajectory (lower panel) of the fluorescence intensity at the spots indicated by the arrows shown in A and B, respectively. The red lines in both panels correspond to each other. The line profiles are well fitted by Gaussian distribution (blue). (E) Histograms of the size of the fluorescent spot calculated from the width of the Gaussian distribution. The red and blue lines indicate the histograms obtained from the TiO_2 nanotubes shown in A and B, respectively. The histogram of the SiO_2 nanotube is also shown for comparison (green).

intensity in the absence (black) and presence (red) of DMSO. By determining the threshold of the fluorescence intensity in the histograms (dotted line), the apparent quantum yield of the generation of $^{\bullet}OH$ in the TiO_2 nanotube[7] can be roughly estimated to be 7.4×10^{-6}, which is significantly larger than that obtained by the bulk experiment (1.1×10^{-8}) (Figure S5, Supporting Information). Moreover, by considering that only the fluorescein present in the TiO_2 nanotube can be detected (Figure S3B, Supporting Information), we expect the quantum yield to be larger than that estimated here. Such a high apparent reaction efficiency as compared to the bulk experiment can be attributed to several effects, such as the low light scattering from the single nanotube, accumulated local concentration of $^{\bullet}OH$,[8] and fast transport process of the reagents (APF) to the active sites during the reaction due to the facility of the diffusion in the pores, which is hindered by the heterogeneities existing in the bulk sample.

To precisely evaluate the transport properties of the porous structures associated with the photocatalytic activity, pores in which fluorescein is generated should be discriminated.

Figure 3A and 3B show TiO_2 nanotubes that exhibit diffusion behavior inherent in the macropore and mesopore, respectively. The figures also show the transmission image (left), fluorescence image (right) captured at the same position, and trajectories of the displacement of the spots indicated by arrows (inset, blue). Because of the scattering of light from the nanotube, the apparent diameter in the transmission image is larger than the actual diameter (ca. 200 nm).

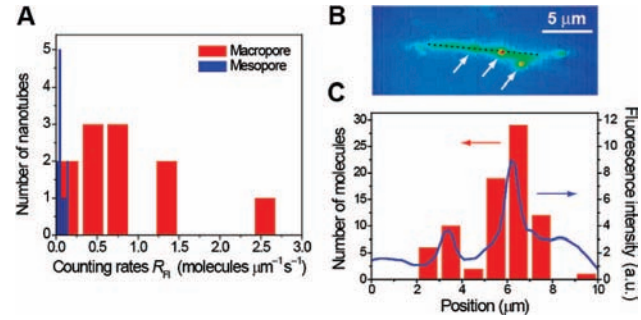

Figure 4. (A) Histograms of the counting rates of single fluorescein molecules, R_{Fl}, in the macropore (red) and mesopore (blue) of the TiO_2 nanotube. (B) The integrated fluorescence intensity of the TiO_2 nanotube (shown in Figure 3A) over 120 s during the photocatalytic reaction. The fluorescence intensity should be directly correlated with the photocatalytically active sites. There are three highly active sites indicated by arrows. (C) Line profile of the integrated fluorescence intensity along the long axis shown by a dotted line in Figure 4B (blue) and the histogram of the number of fluorescein molecules generated at the position, which is determined from the peak of the Gaussian distribution (red).

The trajectory of the fluorescent spot shown in Figure 3A was recorded at only one point because it disappeared in the next acquired image (Figure 3C (bottom), red). Additionally, the width of the line profile of the fluorescent spot shown in Figure 3C (top) is broader than the size of the diffraction-limited spot (ca. 200 nm) commonly observed in the immobilized molecule. These results suggest that the fluorescein shown in Figure 3A is generated in the straight macropore in which the molecule can diffuse freely (diffusion coefficient of fluorescein in solution, $D = 2.8 \times 10^{-10}$ m^2 s^{-1}).[9]

On the other hand, the fluorescent spot shown in Figure 3B represents contrasting results, for example, the trajectory owing to slow diffusion (Figure 3B (inset)), the line profile seen as the diffraction-limited spot (Figure 3D (upper)), and maintenance of the fluorescence intensity for a duration longer than the time resolution of data acquisition (Figure 3D (bottom)). It is also noteworthy that the diffusing molecule mainly exists in a region within an area of ca. 40×40 nm^2, which is of the same order as the wall thickness of the nanotube. The possibility of the adsorption of fluorescein on a TiO_2 particle can be ruled out because of the following reasons: movement of the molecule (Figure 3B), fluorescence quenching due to electron transfer, and electrostatic repulsion between the negatively charged fluorescein and the TiO_2 particle in the phosphate buffer solution (see Supporting Information for details, section 4).[10] Thus, the fluorescein molecule shown in Figure 3B must be present in the mesopores between nanoparticles.[11]

Figure 3E shows histograms of the size of the fluorescent spot calculated from the width of the Gaussian distribution; the results indicate the possibility of diffusion in the pores. The narrow distribution around 230 nm is obtained from the TiO_2 nanotube shown in Figure 3B, corresponding to the mesopore (blue). In contrast, the histogram of the macropore has a peak at around 1 μm and it is broad (red), which can be explained by the residence time of fluorescein in the pores. For example, the average residence time, t_R, is calculated from the spot size and diffusion coefficient in the solution as 450 μs (see Supporting Information for details, section 5). The distributed t_R values are also responsible for the broad distribution of the fluorescence intensity shown in Figure 2C. To examine the specific interaction between the wall of the TiO_2 nanotube and the fluorescein diffusing in the macropore, the result obtained from an SiO_2 nanotube that does not contain the mesopores (Figure S1, Supporting Information) is also shown (Figure 3E, green). In this case, fluorescein was generated by auto-oxidation after intense UV irradiation (Figure S6, Supporting Information). The histograms of both TiO_2 and SiO_2 nanotubes with

a length of ca. 10 μm exibit a similar distribution, confirming that the fluorescein in the macropore of the TiO_2 nanotube diffuses without interaction with the surface, such as adsorption. From the results mentioned above, the photocatalytic activity inherent in the porous structures can be separately estimated.

Figure 4A shows the histograms of the counting rates of single fluorescein molecules, R_{Fl}, measured at the macropore and mesopore, indicating that the average values of R_{Fl} in the pores are 0.85 and 0.065 molecules μm^{-1} s^{-1}, respectively. R_{Fl} of the mesopore is 1 order of magnitude smaller than that of the macropore, despite the possible advantage that its small volume facilitates the accumulation of •OH; this strongly indicates the effect of the kinetics of the transport of reagents on the photocatalytic activity, which is not evident in the bulk measurement (Figure S5, Supporting Information). As a next step, we have attempted to study the spatial heterogeneity of active sites on individual TiO_2 nanotubes.

Figure 4B shows the integrated fluorescence intensity over 120 s arising from the fluorescein generated on the surface of TiO_2 nanotube during the photocatalytic reaction; this should reveal the active sites distributed over the nanotube, where the photocatalytic reaction occurs efficiently. Interestingly, it was found that there are three highly active sites on the nanotube, as indicated by the arrows. To confirm that these sites are not due to the enhanced light scattering arising from the existence of cracks or branches on the nanotube, the histogram of the number of fluorescein molecules counted along the dotted line in Figure 4B was carefully examined, as shown in Figure 4C (red). In this case, the precise position at which fluorescein is generated is determined from the Gaussian fits to the fluorescence intensity profiles of fluorescein that disappeared immediately by fast diffusion (Figure 3C, upper). For the sake of comparison, the line profile of the integrated fluorescence intensity is also shown in Figure 4C (blue). The fact that the peaks in both profiles approximately correspond to each other reveals the heterogeneous distribution of the active sites even in the isolated nanotube. The origin of the observed heterogeneity has not yet been fully explained; however, it is possibly attributed to the intrinsic distribution of surface defects such as oxygen vacancies that are present in the respective nanotubes,[12] which should mediate the electron transfer from the conduction band to O_2, thus leading to the generation of H_2O_2 as the precursor of •OH.[13] To clarify the relationship between the distributions of (photo)catalytically active sites and surface defects, however, further studies are required to also consider the direct observation of defect-mediated photoluminescence at the single-nanotube level, which we have recently developed.[14]

In conclusion, we have investigated the photocatalytic activity of individual porous TiO_2 nanotubes by the single-molecule counting of •OH using a specific fluorescent probe. The time- and space-resolved observation of emissive fluorescein generated by the photocatalytic reaction clearly reveals that the transport of reagents inherent in the porous structures is closely related to the photocatalytic activity. Furthermore, we discovered the spatial heterogeneity of reactive sites in an isolated TiO_2 nanotube for the first time. Experiments on a single nanotube provide information that is useful for elucidating the reaction mechanism of the heterogeneous (photo)catalyst and for designing advanced porous materials.

Acknowledgment. This study was partly supported by a Grant-in-Aid for Scientific Research (Projects 17105005, 19750115, and others) from the Ministry of Education, Culture, Sports, Science and Technology (MEXT) of the Japanese Government. T.T. is thankful for the partial support provided by the Iketani Science and Technology Foundation. K.N. expresses his thanks for the JSPS Research Fellowship for Young Scientists and to the Global COE Program "Global Education and Research Center for Bio-Environmental Chemistry" of Osaka University.

Supporting Information Available: Movies for the macropores and mesopores (avi files); experimental details, control experiments, and additional discussions. This material is available free of charge via the Internet at http://pubs.acs.org.

References

(1) For example: *Handbook of Porous Solids*; Schüth, F., Sing, K. S. W., Weitkamp, J., Eds.; Wiley-VCH: Weinheim, Germany, 2002.
(2) (a) Chen, X.; Mao, S. S. *Chem. Rev.* **2007**, *107*, 2891–2959. (b) Shiraishi, Y.; Saito, N.; Hirai, T. *J. Am. Chem. Soc.* **2005**, *127*, 12820–12822. (c) Li, H.; Bian, Z.; Zhu, J.; Zhang, D.; Li, G.; Huo, Y.; Li, H.; Lu, Y. *J. Am. Chem. Soc.* **2007**, *129*, 8406–8407. (d) Pan, J. H.; Zhang, X.; Du, A. J.; Sun, D. D.; Leckie, J. O. *J. Am. Chem. Soc.* **2008**, *130*, 11256–11257. (e) Lakshmi, B. B.; Dorhout, P. K.; Martin, C. R. *Chem. Mater.* **1997**, *9*, 857–862. (f) Macak, J. M.; Zlamal, M.; Krysa, J.; Schmuki, P. *Small* **2007**, *3*, 300–304.
(3) (a) Paulose, M.; Prakasam, H. E.; Varghese, O. K.; Peng, L.; Popat, K. C.; Mor, G. K.; Desai, T. A.; Grimes, C. A. *J. Phys. Chem.C* **2007**, *111*, 14992–14997. (b) Yang, S.-C.; Yang, D.-J.; Kim, J.; Hong, J.-M.; Kim, H.-G.; Kim, I.-D.; Lee, H. *Adv. Mater.* **2008**, *20*, 1059–1064. (c) Mor, G. K.; Varghese, O. K.; Paulose, M.; Shankar, K.; Grimes, C. A. *Sol. Energy Mater. Sol. Cells* **2006**, *90*, 2011–2075. (d) Park, J. H.; Kim, S.; Bard, A. J. *Nano Lett.* **2006**, *6*, 24–28.
(4) For example: Roeffaers, M. B. J.; Sels, B. F.; Uji-i, H.; De Schryver, F. C.; Jacobs, P. A.; De Vos, D. E.; Hofkens, J. *Nature* **2006**, *439*, 572–575. (b) Martı´nez, V. M.; De Cremer, G.; Roeffaers, M. B. J.; Sliwa, M.; Baruah, M.; De Vos, D. E.; Hofkens, J.; Sels, B. F. *J. Am. Chem. Soc.* **2008**, *130*, 13192–13193. (c) Xu, W.; Kong, J. S.; Yeh, Y.-T. E.; Chen, P. *Nat. Mater.* **2008**, *7*, 992–996.
(5) Imai, H.; Takei, Y.; Shimizu, K.; Matsuda, M.; Hirashima, H. *J. Mater. Chem.* **1999**, *9*, 2971–2972.
(6) (a) Setsukinai, K.; Urano, Y.; Kakinuma, K.; Majima, H. J.; Nagano, T. *J. Biol. Chem.* **2003**, *278*, 3170–3175. (b) Naito, K.; Tachikawa, T.; Fujitsuka, M.; Majima, T. *J. Phys. Chem. C* **2008**, *112*, 1048–1059.
(7) The actual quantum yield of the generation of •OH in the TiO_2 nanotube must be defined as the ratio of the number of generated fluorescein molecules (N_{Fl}) to the number of photons absorbed by the TiO_2 nanotube (N_{abs}), N_{Fl}/N_{abs}. However, because of the difficulty of measuring the absolute number of absorbed photons because of light scattering at the TiO_2 surface, instead of the number of absorbed photons, the number of photons irradiated on the TiO_2 nanotube (N_{TiO2}) is used to estimate the photocatalytic activity of the TiO_2 nanotube. Here, such quantum efficiency is called as the apparent quantum efficiency (see Supporting Information for details, section 6).
(8) (a) As reported elsewhere, •OH is trapped on the TiO_2 surface and is converted to a less-active surface •OH with a nearly diffusion-controlled rate;[8b,c] this indicates that the •OH generated in the macropore and mesopore scarcely diffuses out of the pores, and hence, the equilibrium concentration of •OH in the nanotube under UV irradiation depends on the local concentration of the precursor H_2O_2 molecules in the pores. Thus, the photocatalytic activity of the TiO_2 nanotube must be closely related to the pore size of its porous structures that determine the accumulated concentration of H_2O_2. (b) Lawless, D.; Serpone, N.; Meisel, D. *J. Phys. Chem.* **1991**, *95*, 5166–5170. (c) Tojo, S.; Tachikawa, T.; Fujitsuka, M.; Majima, T. *Chem. Phys. Lett.* **2004**, *384*, 312–316.
(9) Chattopadhyay, K.; Saffarian, S.; Elson, E. L.; Frieden, C. *Proc. Natl. Acad. Sci. U.S.A.* **2002**, *99*, 14171–14176.
(10) Wu, H.-P.; Cheng, T.-L.; Tseng, W.-L. *Langmuir* **2007**, *23*, 7880–7885.
(11) (a) It should be noted that the different diffusion behavior of fluorescein molecules in each TiO_2 nanotube intrinsic to either the macropore or mesopore is possibly due to the structural heterogeneities, such as the distributions of the diameter of the macropore and the thickness of walls containing the mesopores, which cannot be addressed by the wide-field fluorescence imaging. To clarify the relationship between the diffusion behavior of reagents and the structure of nanotubes at the nanometer scale, a combination of fluorescence imaging and TEM or AFM analysis on a single nanotube is required.[11b] For example: (b) Zürner, A.; Kirstein, J.; Döblinger, M.; Bräuchle, C.; Bein, T. *Nature* **2007**, *450*, 705–708.
(12) (a) Dimitrijevic, N. M.; Saponjic, Z. V.; Rabatic, B. M.; Rajh, T. *J. Am. Chem. Soc.* **2005**, *127*, 1344–1345. (b) Kolmakov, A.; Potluri, S.; Barinov, A.; Menteş, T. O.; Gregoratti, L.; Ninõ, M. A.; Locatelli, A.; Kiskinova, M. *ACS Nano* **2008**, *2*, 1993–2000.
(13) For example: (a) Thompson, T. L.; Yates, J. T., Jr *Chem. Rev.* **2006**, *106*, 4428–4453. (b) Tachikawa, T.; Fujitsuka, M.; Majima, T. *J. Phys. Chem. C* **2007**, *111*, 5259–5275.
(14) Tachikawa, T.; Ishigaki, T.; Li, J.-G.; Fujitsuka, M.; Majima, T. *Angew. Chem., Int. Ed.* **2008**, *47*, 5348–5352.

JA808335B